HHS Public Access

Author manuscript

Neuron. Author manuscript; available in PMC 2017 April 20.

Published in final edited form as:

Neuron. 2016 April 20; 90(2): 333–347. doi:10.1016/j.neuron.2016.03.028.

Cholinergic Mesopontine Signals Govern Locomotion and Reward Through Dissociable Midbrain Pathways

Cheng Xiao[1], **Jounhong Ryan Cho**[2], **Chunyi Zhou**[1], **Jennifer B. Treweek**[1], **Ken Chan**[1], **Sheri L. McKinney**[1], **Bin Yang**[1], and **Viviana Gradinaru**[1,*]

[1]Division of Biology and Biological Engineering, California Institute of Technology, Pasadena, California 91125, USA

[2]Computation and Neural Systems, California Institute of Technology, Pasadena, California 91125, USA

Abstract

The mesopontine tegmentum, including the pedunculopontine and laterodorsal tegmental nuclei (PPN and LDT), provides major cholinergic inputs to midbrain and regulates locomotion and reward. To delineate the underlying projection-specific circuit mechanisms we employed optogenetics to control mesopontine cholinergic neurons at somata and at divergent projections within distinct midbrain areas. Bidirectional manipulation of PPN cholinergic cell bodies exerted opposing effects on locomotor behavior and reinforcement learning. These motor and reward effects were separable via limiting photostimulation to PPN cholinergic terminals in the ventral substantia nigra pars compacta (vSNc) or to the ventral tegmental area (VTA), respectively. LDT cholinergic neurons also form connections with vSNc and VTA neurons, however although photo-excitation of LDT cholinergic terminals in the VTA caused positive reinforcement, LDT-to-vSNc modulation did not alter locomotion or reward. Therefore, the selective targeting of projection-specific mesopontine cholinergic pathways may offer increased benefit in treating movement and addiction disorders.

Keywords

mesopontine tegmentum; pedunculopontine nucleus; laterodorsal tegmental nucleus; cholinergic neuron; substantia nigra pars compacta; ventral tegmental area; locomotion; conditioned place preference; optogenetics; retrograde tracing

*To whom correspondence should be addressed: Viviana Gradinaru, Ph.D., Division of Biology and Biological Engineering, California Institute of Technology, 1200 East California Blvd. MC 156-29, Pasadena, CA 91125, Phone: (626) 395-6813, viviana@caltech.edu.

Author Contributions:

C.X. and V.G. designed the project. C.X., R.C., C.Z., J.T., and V.G. planned experiments and analyzed data. C.X., R.C., C.Z., S.L.M. and J.T. collected data. K.C. contributed to animal behavior tests and data illustration. B.Y. provided training in histology and image processing. C.X. and V.G. wrote the manuscript with help from co-authors. Each author read and approved the final manuscript. VG supervised all aspects of the project.

Introduction

The pedunculopontine nucleus (PPN) is a heterogeneous brainstem structure that contains cholinergic (ChAT), glutamatergic, and GABAergic neurons (Benarroch, 2013; Jenkinson et al., 2009). Accumulating evidence suggests that PPN ChAT neurons play key roles in both motor and non-motor behaviors (Morita et al., 2014). Parkinson's disease patients with gait disorders and postural instability display degeneration of the PPN ChAT neurons, and the severity of balance deficits is correlated with a reduction in PPN ChAT-neuron numbers and activity (Bohnen et al., 2013; Bohnen et al., 2009). In parkinsonian non-human primate models, chemical lesion of PPN ChAT neurons is necessary and sufficient to impair gait and balance (Karachi et al., 2010). In addition to affecting motor behavior, ChAT-neuron-selective chemical lesions of the PPN also affect drug-seeking behavior (Lanca et al., 2000). These studies suggest that PPN ChAT neurons are instrumental for normal function in movement and reward reinforcement; however, they do not identify the downstream effectors.

The PPN projects to multiple targets in the basal ganglia, midbrain, cerebellum, thalamus, and the reticular formation (Ballanger et al., 2009; Benarroch, 2013; Dautan et al., 2014; Jenkinson et al., 2009; Marani et al., 2008). Although electrically and pharmacologically stimulating PPN neurons *in vivo* leads to overall excitatory outcomes in downstream nuclei (Ballanger et al., 2009; Blaha et al., 1996), the projections from the PPN to individual downstream neurons are complex. Two notable targets of PPN ChAT circuitry, the substantia nigra pars compacta (SNc) and the ventral tegmental area (VTA), are implicated in locomotion and reward processing (Bermudez and Schultz, 2014; Bromberg-Martin et al., 2010; Ikemoto, 2007; Lerner et al., 2015; Roeper, 2013). ChAT, glutamatergic, and GABAergic neurons of the PPN form convergent connections onto SNc and VTA neurons, but their synaptic contacts with individual neurons are often non-overlapping (Futami et al., 1995; Good and Lupica, 2009; Scarnati et al., 1986). The multifaceted roles of SNc and VTA neurons in exploratory activity, habituation, reinforcement, aversion (Bromberg-Martin et al., 2010; Friedman et al., 2014; Lerner et al., 2015; Roeper, 2013; Walsh et al., 2014), and the involvement of multiple nuclei in locomotion and reward (Benarroch, 2013; Bromberg-Martin et al., 2010; Ikemoto, 2007; Jenkinson et al., 2009; Kravitz and Kreitzer, 2012) adds experimental complexity to the assessment of how PPN ChAT tone in the VTA and SNc patterns goal-directed behaviors. Whether selectively and temporarily enhancing the tonic activity of PPN ChAT neurons, without affecting PPN glutamatergic and GABAergic neurons, is sufficient to recruit SNc and VTA neurons and to regulate the aforementioned behaviors is unknown. A strategy that enables specific modulation of ChAT projections without perturbing glutamatergic and GABAergic projections can facilitate both *in vitro* and *in vivo* characterization of ChAT circuitry originated in the PPN.

To dissect out the behavioral effect of ChAT signaling along each PPN-to-midbrain circuit, we have employed optogenetic tools (Gradinaru et al., 2009; Gradinaru et al., 2010; Hausser, 2014; Walsh et al., 2014) and ChAT-Cre rats (Witten et al., 2011). Electrical and chemical interventions, which are commonly used to study the anatomy and physiology of the PPN, do not offer the spatiotemporal or cell-type specificity required to selectively harness specific PPN ChAT projections to the VTA and SNc, or to examine differences in PPN cell

connectivity with SNc and VTA nuclei. Highlighting the requirement for precise spatial targeting of neuronal manipulations, it is noteworthy that the dorsal and ventral tiers of the SNc (dSNc and vSNc) project to distinct sub-regions of the striatum and may have differential vulnerability to neurodegenerative assaults (Hassan and Benarroch, 2015). Thus they merit investigation as separate subnuclei.

We found that optogenetic modulation of PPN ChAT somata altered both motor activity and reward reinforcement, whereas targeted photo-stimulation of PPN ChAT terminals in the vSNc or VTA granted separable control of these physiological processes. Importantly, these results do not rule out cholinergic control of midbrain functions from non-PPN sources. Indeed, as shown before (Chen and Lodge, 2013; Lodge and Grace, 2006; Mena-Segovia et al., 2008) and confirmed here, ChAT neurons in the laterodorsal tegmental nucleus (LDT), also formed functional connections with midbrain neurons. While photo-excitation of these connections in the VTA regulated reward reinforcement, photoexcitation of LDT ChAT terminals in the vSNc did not alter locomotion, which contrasts with the effects of PPN originating cholinergic modulation. Therefore, ChAT projections from the PPN and the LDT to the vSNc and VTA play distinct roles in regulating motor and reward behaviors, and could be refined therapeutic targets for movement disorder and drug addiction.

Results

Previous studies (Benarroch, 2013; Jenkinson et al., 2009; Mena-Segovia et al., 2008; Oakman et al., 1995) have demonstrated connections between PPN neurons and SNc/VTA neurons by neuronal tracing and electrophysiological techniques. As these techniques often lacked cell specificity, ChAT connections were neither imaged in intact form nor were they selectively stimulated without also perturbing glutamatergic and GABAergic connections. We injected adeno-associated virus serotype 5 (AAV5) carrying Cre-dependent (DIO; double-floxed inverse open reading frame) ChR2-eYFP into the PPN of ChAT-Cre rats to selectively label ChAT neurons and their projections (Fig. 1A). To visualize the projections to the SNc and VTA, we used PACT clearing (Treweek et al., 2015; Yang et al., 2014) for facile and accurate mapping of dense, long-range fibers in 1 – 2 mm thick brain sections. We observed ChR2-eYFP labeled axonal fibers from PPN ChAT neurons within both the dorsal and ventral tiers of the SNc (dSNc and vSNc) as well as within the VTA (Fig. 1B, C).

We confirmed the functional properties of these connections by performing whole-cell patch-clamp recordings from SNc and VTA neurons adjacent to ChR2-expressing PPN ChAT axonal fibers in live midbrain slices of ChR2-injected rats (Fig. 1D). ChAT neurons usually form connections with downstream neurons through non-synaptic volume transmission (Miwa et al., 2011). Since ACh released in response to a short stimulation epoch is rapidly hydrolyzed by acetylcholinesterase before reaching its receptors, long stimulation epochs are necessary in order for ACh to accumulate and subsequently activate ACh receptors. Therefore, to increase our probability of detecting existing functional ChAT transmission, we applied 5 – 10 s continuous blue light stimulation (Fig. 1E–G). Under these conditions, we detected inward currents in 33%, 24%, and 44% of vSNc, dSNc, and VTA neurons, respectively (Fig. 1E–I). Meanwhile, blue light accelerated neuronal firing (Fig.

1E–G, J). These data suggest that PPN ChAT neurons form excitatory connections with SNc and VTA neurons.

Midbrain neurons contain both nicotinic and muscarinic ACh receptors (nAChRs and mAChRs) (Drenan and Lester, 2012; Miwa et al., 2011; Yeomans, 1995), and either is capable of mediating the response to light-induced ChAT release. We observed photocurrents that were not significantly changed by atropine, a mAChR antagonist, but that were significantly blocked by mecamylamine (MEC), a nAChR antagonist (Fig. 1K; Fig. S1A, D); furthermore, MEC also blocked the enhancement of firing in response to photo-excitation (Fig. 1E). These data suggest that nAChRs predominantly mediate the connectivity between PPN ChAT neurons and SNc/VTA neurons.

Given that nAChRs modulate neurotransmitter release in midbrain (Dani and Bertrand, 2007), the nAChRs that mediate the photocurrents could be located on the recorded neurons or on afferent terminals releasing other neurotransmitters, such as, glutamate or GABA. To define where these nAChRs are located, we further characterized the pharmacological properties of the photocurrents. We observed that bicuculline (10 μM, Bic), a $GABA_A$ receptor blocker, did not affect the photocurrents in midbrain neurons, but 10 μM MEC blocked these currents (Fig. 1K; Fig. S1B, E). In some midbrain neurons (8/18), the photocurrents were completely blocked by glutamate receptor antagonists (APV and CNQX); whereas, in other neurons (10/18), the combined application of APV and CNQX only partially reduced the currents, and MEC blocked the remaining currents (Fig. 1K; Fig. S1C, F). These results suggest that nAChRs both in afferent glutamatergic terminals and in midbrain neurons are important targets of endogenously released ACh from PPN.

The above optogenetic tracing data (Fig. 1B, C) support the hypothesis that the SNc and VTA are downstream targets of PPN ChAT neurons. Since the SNc and VTA are involved in locomotion and reward reinforcement (Bromberg-Martin et al., 2010; Lerner et al., 2015; Maskos, 2008; Patterson et al., 2015; Roeper, 2013), it follows that PPN ChAT activity may impact locomotion and reward reinforcement. To test this hypothesis, we selectively and reversibly manipulated opsin-expressing PPN ChAT neurons in freely behaving rats.

Similar to previous studies (Jenkinson et al., 2009), our data illustrate that ChAT neurons reside throughout the PPN and account for almost half of all neurons in both the rostral and caudal PPN (Fig. 2A, B; Fig. S2A). To tailor practical optogenetic stimulation paradigm (i.e. duration and frequency) to modulate neurons within their spiking capability, we therefore characterized the biophysical properties of PPN ChAT neurons using brain-slice patch-clamp recordings (Fig. 2C–H). Most PPN neurons fired spontaneously at <10 Hz (Fig. S2B). When increasing steps of depolarizing current were injected into PPN neurons, the firing rates of ChAT neurons increased more than non-ChAT neurons (Fig. 2E, Tab S1), consistent with our data showing that ChAT neurons had higher input resistance (Fig. 2F). The optimal stimulation duration to evoke reliable single action potential for PPN neurons was 10 ms (Fig. 2G, H; Fig. S2C, D; Tab S2). Thus, we applied 10 ms light pulses to evoke action potentials in the following *ex vivo* and *in vivo* experiments involving optogenetic excitation.

To achieve optogenetic control of PPN ChAT neurons we stereotaxically delivered AAV5-DIO- ChR2-eYFP or Arch3.0-eYFP genes into the PPN of ChAT-Cre rats (Chow et al., 2010; Mattis et al., 2012; Witten et al., 2011) (Fig. 3A–C, I–K; Fig. 4A). Whole-cell patch-clamp recordings in PPN brain slices (Fig. S3A, D) confirmed functional expression levels of virally transduced ChR2 and Arch3 in PPN neurons: blue and green light stimulation evoked robust photocurrents in recorded cells (Fig. 3D, L; Fig. S3C, E, F) and effectively modified the firing patterns (Fig. 3E, L). Opsin expression was specific to ChAT neurons (Fig. 3C, K). Additionally, blue light pulses (10 ms) reliably evoked inward currents (Fig. S3E) and action potentials (Fig. 3E–H) in PPN ChAT neurons expressing ChR2 (Fig. S3A).

To understand the behavioral contributions of PPN ChAT neurons, we monitored freely moving rats for changes in locomotor activity in response to photo-modulation of opsin-expressing PPN ChAT neurons. For photo-excitation, we applied 20 Hz stimuli (Fig. 4A; Fig. S4A) because: 20 Hz is higher than the average spontaneous firing rates (<12 Hz) of PPN neurons shown in our *in vitro* data (Fig. S2B; Tab S1) and in previous *in vivo* studies (Norton et al., 2011), and 20 Hz is within the frequency range (20–25Hz) used for electrical stimulation of the PPN and prior photo-excitation (at 20Hz) of PPN ChAT neurons that effectively enhances movement (Benarroch, 2013; Jenkinson et al., 2009; Plaha and Gill, 2005; Roseberry et al., 2016; Stefani et al., 2007). To quantify locomotor behavior, we used an open field test (see Methods). Exposure to ChR2-activating blue light (20 Hz, 10 ms pulse width) robustly and reversibly increased locomotion (Fig. 4B, Fig. S4D). Moreover, the enhancement of locomotion during photo-excitation was abolished by MEC (2 mg/kg, i.p.) (Fig. S4G–I). These data indicate that increased PPN ChAT activity is sufficient to promote locomotion by enhanced activation of nAChRs. To test whether spontaneous firing in PPN ChAT neurons is necessary to maintain normal locomotion, we photo-inhibited Arch3-expressing PPN ChAT neurons with continuous green light during open field tests. Photo-inhibition significantly reduced locomotor activity, and this effect reversed upon light termination (Fig. 4C, Fig. S4J). Neither blue nor green light stimulation altered locomotion in control mCherry rats (Fig. 4B, C; Fig. S4B, D, J), eliminating the possibility that virus transduction or light stimulation exerted non-specific actions on locomotion. During testing, ChR2, Arch3 and corresponding mCherry cohorts exhibited similar levels of baseline activity (Fig. S4E, K). These data provide a causal link between the activity of PPN ChAT neurons and locomotion.

The PPN contains neurons that respond to either movement or reward signals, as shown by prior *in vivo* single-unit recordings (Lau et al., 2015; Norton et al., 2011; Okada and Kobayashi, 2013). Given that ChAT neurons are a dominant neuronal population in the PPN (Fig. 2B), and that PPN neuronal activity has been linked to numerous physiological functions, our optogenetic modulation of ChAT-neuron activity could affect non-motor behaviors as well. To confirm the hypothesized role of PPN ChAT signaling in reward processing, we used a conditioned place preference (CPP) paradigm (Fig. 4D, see supplementary materials) to test whether photo-excitation and photo-inhibition of PPN ChAT neurons during place conditioning would induce place preference and aversion, respectively (Fig. 4E). On the first day, the rats preferred the dark compartment (350 – 550 s) to the white compartment (50 – 250 s) (Fig. S5A). Therefore, we applied a biased light-conditioning paradigm on the following four consecutive days. Since lesioning PPN ChAT

neurons reduces nicotine self-administration (Lanca et al., 2000), we hypothesized that exciting and inhibiting PPN ChAT neurons would cause positive and negative reinforcement, respectively. In a CPP paradigm, the time spent in the light-paired side should increase in response to PPN ChAT photo-excitation but decrease with PPN ChAT photo-inhibition. To avoid ceiling and floor effects for conditioning, we paired ChR2 rats with blue light pulses in the non-preferred (white) compartment and Arch3 rats with green light in preferred (dark) compartment (Fig. 4E). As controls, we paired mCherry rats with blue light pulses in the white compartment and with green light in the dark compartment (Fig. 4E). After light-conditioning, ChR2 rats exhibited a statistically significant increase in the time spent in the compartment paired with photo-excitation (Fig. 4F, G), whereas Arch3 rats displayed a significant reduction in the time spent in the compartment paired with photo-inhibition (Fig. 4H, I). Therefore, modulation of PPN ChAT somata is also sufficient to bidirectionally affect reward processing. Note that four days of light-conditioning had only minor effects on locomotion in the post-conditioning session (Fig. S5B, C).

Based on our findings that optogenetic modulation of PPN ChAT neurons modifies both motor and reward behaviors, we reasoned that the downstream targets of ChAT projections may be involved in conveying these behaviors. To understand the role of PPN projections to the SNc and VTA in controlling locomotion and reward *in vivo*, we restricted optogenetic modulation to ChAT axon terminals in the vSNc (Fig. 5A, B, Fig. S6A–C) and VTA (Fig. 6A, B; Fig. S7A–C). We chose to target vSNc-projecting and not dSNc-projecting fibers as the smaller size of the vSNc and its anatomical segregation from the VTA and dSNc (Fig. 1B; Fig. 5A, B) facilitate its optogenetic isolation and recruitment.

In the open field test, photo-excitation of PPN-to-vSNc projections increased locomotion (Fig. 5C, D; Fig. S6D). Photo-excitation of terminals could potentially cause back-propagating action potentials (Jennings et al., 2013) in the vSNc projecting PPN ChAT neurons and recruit downstream nuclei other than the vSNc, with the PPN-to-vSNc connection playing only a minor role. To ensure that the vSNc was indeed a key contributor, we photo-inhibited the projections of PPN ChAT neurons to the vSNc in rats injected with AAV5-DIO-Arch3.0-eYFP in the PPN (Fig. 5A; Fig. S6C) and observed reduced locomotion (Fig. 5E, F; Fig. S6E), confirming the critical role of this connection in motor control. Photo-excitation of the PPN-to-vSNc projections had no effect on CPP (Fig. 5G, H).

In contrast to PPN-to-vSNc projections, photo-excitation of PPN-to-VTA projections did not change locomotion in the open field test (Fig. 6C, D; Fig. S7A, B), but did attenuate place aversion to the previously non-preferred compartment (Fig. 6E, F) in CPP. This effect could be related to increased activity of VTA neurons (Fig. S7F–H), because direct stimulation of VTA neurons is sufficient to cause reward reinforcement (Tsai et al., 2009). We next tested whether photo-inhibition of PPN-to-VTA projections has opposite effects compared with photo-excitation of the projections. Since Arch3.0 can have limitations for long epoch terminal inhibition (Mahn et al., 2016), we virally transduced eNpHR3.0-eYFP into PPN ChAT neurons and utilized green-light to inhibit the terminals of these neurons (Fig. 6A; Fig. S7C–E). Conditioning eNpHR3.0-injected rats with photo-inhibition of PPN-to-VTA projections reduced time spent in the light-paired compartment (Fig. 6G, H).

Collectively, the above data indicate that targeted optogenetic modulation of PPN ChAT terminals located in the vSNc and VTA bidirectionally affected locomotion and reward reinforcement, respectively. In addition to the PPN, midbrain neurons also receive cholinergic signaling from the LDT (Hassan and Benarroch, 2015; Maskos, 2008; Mena-Segovia et al., 2008). Previous studies reveal that LDT ChAT neurons project preferentially to the VTA and sparsely to the SNc (Hassan and Benarroch, 2015; Mena-Segovia et al., 2008). However, it is still an open question whether the ChAT projections from the LDT to the midbrain have similar functions to those from the PPN. To answer this question, we performed photo-excitation of LDT ChAT terminals in both the VTA and vSNc. We delivered AAV5-DIO-ChR2-eYFP to the LDT of ChAT-Cre rats; 66% (368/556) of ChAT neurons contained ChR2 (Fig. 7A, B). In brain slices, photo-excitation of ChR2-eYFP expressing LDT ChAT somata evoked inward currents and action potentials (Fig. 7C); when applied to LDT ChAT terminals, blue light evoked inward currents in 22, 18, and 33% of vSNc, dSNc and VTA neurons, respectively (Fig. 7D, E, F). These proportions were similar to those of midbrain neurons responding to PPN ChAT terminal stimulation (Fig. 1H, Fig. 7F). We observed that APV+CNQX partially blocked the photocurrents in 5/10 neurons, but did not change the photocurrents in 5/10 neurons. Meanwhile, Bic did not reduce photocurrents in all 4 neurons we recorded. All of the remaining currents were eliminated by MEC (Fig. 7G; Fig. S8C, D). These pharmacological properties are similar to the photocurrents in response to photo-excitation of PPN ChAT terminals in midbrain except that nAChRs on glutamatergic terminals had less contribution to these photocurrents (Fig. 7G vs. Fig. 1K).

The above electrophysiological data indicate that the LDT and PPN ChAT neurons may have similar projections to the vSNc and VTA and therefore mediate similar behavioral outputs. We performed photo-excitation of LDT ChAT terminals in the vSNc and VTA to test whether the modulation leads to behavioral results similar to photo-excitation of PPN ChAT terminals. In open field tests, photo-excitation of neither LDT-to-VTA nor LDT-to-vSNc ChAT terminals altered locomotion (Fig. 7I, M), in contrast to the involvement of PPN-to-vSNc projections in locomotion. In CPP assays, conditioning the rats with photo-excitation of LDT-to-VTA ChAT projections (Fig. 7H; Fig. S8A) increased the time spent in the light-paired compartment (Fig. 7J, K), while shining blue light on LDT-to-vSNc projections (Fig. 7L; Fig. S8B) to condition ChR2 and eYFP rats caused similar changes in their place preference (Fig. 7N, O). The results suggest that the PPN and LDT sends similar ChAT projections to the VTA regulating reward processing; in contrast to the PPN, LDT ChAT signaling to the vSNc did not alter locomotion.

To map the PPN and LDT ChAT projections to the VTA and vSNc, we injected retrograde herpes simplex viral (HSV) vectors carrying mCherry- and eYFP-Cre (Antinone and Smith, 2010; Nieh et al., 2015), respectively, into the vSNc and VTA (Fig. 8A). The virus is taken up by terminals and transported along the axons to the somata, thereby labeling upstream neurons in the PPN and LDT. In both the PPN and LDT, VTA and vSNc projecting ChAT neurons and non-ChAT neurons were intermingled (Fig. 8B, C). The summarized data (Fig. 8D) show that more ChAT neurons projected to the vSNc (PPN: 58%; LDT: 29%) than to the VTA (PPN: 20%; LDT: 25%), and 14% of ChAT neurons in both the PPN and LDT projected to both the vSNc and VTA. Compared with the LDT (Fig. 8D), the PPN had

significantly higher percentage of ChAT neurons projecting to either the vSNc, the VTA, or both (64% vs. 40%), higher percentage of vSNc projecting neurons (58% vs. 29%), but lower percentage of VTA projecting ChAT neurons (20% vs. 25%). The PPN and LDT had similar percentage of ChAT neurons projecting to both the VTA and vSNc (~ 14%) (Fig. 8 D). Consistent with previous studies (Lammel et al., 2012; Mena-Segovia et al., 2008), ChAT neurons are not the only neuron population in the PPN and LDT projecting to the vSNc and VTA (Fig. 8B, C; Fig. S8E). Interestingly, a great majority of vSNc and a minority of VTA projecting neurons were cholinergic (Fig. S8E).

To clarify whether the projections from these two groups of ChAT neurons are intermingled in the vSNc and VTA, we delivered AAV5-DIO-eYFP in the PPN and AAV5-DIO-mCherry in the LDT to trace these projections (Fig. S8F). We observed that the ChAT fibers were adjacent to each other in both the vSNc and VTA (Fig. S8G). Interestingly, in the vSNc, PPN ChAT fibers significantly outnumbered LDT fibers, which is consistent with the retrograde tracing results and the differential roles observed in locomotion tests.

Discussion

The PPN contains heterogeneous cell populations with divergent brain-wide projections (Benarroch, 2013; Jenkinson et al., 2009; Mena-Segovia et al., 2008; Morita et al., 2014). It is implicated in a broad spectrum of behaviors, including locomotion, reward, and sleep (Arnulf et al., 2010; Benarroch, 2013; Maskos, 2008). The link between the PPN and these behaviors has mostly been obtained through neuromodulation with non-cell-specific pharmacological tools, electrical stimulation, and chemical lesions. Optogenetics (Gradinaru et al., 2009; Gradinaru et al., 2010; Hausser, 2014; Walsh et al., 2014) and chemogenetics (Sternson and Roth, 2014; Urban and Roth, 2015) provide tools that enable dissection of heterogeneous PPN circuits at the level of individual neuronal types. A few studies have taken advantage of these techniques to selectively enhance the activity of PPN ChAT neurons, from which it was observed that PPN ChAT neurons significantly modulate sleep (Van Dort et al., 2015) and motor functions (Pienaar et al., 2015; Roseberry et al., 2016). However, the behavioral effects of modulating PPN ChAT activity in opposing directions had yet to be explored.

We applied optogenetics to selectively target and bidirectionally modulate PPN ChAT neurons both at the somata and at the terminals, and further characterize the projections from these neurons to midbrain areas. First, we employed techniques that enable intact visualization of large tissue volume with high resolution (PACT (Treweek et al., 2015; Yang et al., 2014), Fig. 1B–C) and imaged the projections of PPN ChAT neurons to midbrain nuclei. Second, using retrograde HSV, we revealed that PPN ChAT neurons projecting to the VTA and vSNc are intermingled, and some neurons project to both the VTA and vSNc besides separate, parallel projections (Fig. 8B–D). Third, in acute brain slices, we applied optogenetics to stimulate endogenous ACh release which evoked non-synaptic responses in midbrain neurons through activating nAChRs in the recorded neurons and glutamate terminals (Fig. 1D–K; Fig. S1). Although some PPN ChAT neurons have been reported to contain glutamatergic and/or GABAergic marker proteins, it remains controversial whether these neurotransmitters are co-released from the terminals (Benarroch, 2013; Jenkinson et

al., 2009; Mena-Segovia et al., 2008; Roseberry et al., 2016; Wang and Morales, 2009). In our experiments, the extensive current attenuation by MEC (Fig. 1E–G, J; Fig. S1) suggests that ACh is the main underlying neurotransmitter and co-release of other neurotransmitters (e.g. glutamate or GABA) plays a minor, if any, role in PPN ChAT terminals in the midbrain, consistent with previous studies (Roseberry et al., 2016; Wang and Morales, 2009).

PPN neurons are known to modulate motor behaviors. Electrical and chemical stimulation of the PPN enhance locomotion (Jenkinson et al., 2004), and nonspecific chemical lesion of the PPN leads to hypokinesia (Kojima et al., 1997; Masdeu et al., 1994). Moreover, direct *in vivo* electrophysiological recordings have shown that during voluntary movement (Jenkinson et al., 2009), imaginary motion, and passive movement (Tattersall et al., 2014), PPN neurons exhibit disparate changes (increased, decreased, or unchanged) in firing rates. These studies suggest that subsets of PPN neurons may be involved in motor control. We observed that photo-excitation of PPN ChAT neurons (20 Hz) caused hyperactivity (Fig. 4B) whereas photo-inhibition caused hypokinesia (Fig. 4C). Furthermore, the hyperactivity evoked by PPN ChAT-neuron stimulation was blocked by MEC (Fig. S4H,I), again suggesting either that these neurons do not co-release glutamate or that any co-released glutamate plays only a minor role in this behavior. These results demonstrate that bidirectional modulation of PPN ChAT neurons is sufficient to regulate locomotion and may be a potential therapeutic target for movement disorders involving both hypokinesia and involuntary movement.

In addition to locomotion, the PPN is also involved in reward processing: PPN neuronal activity changes in response to reward signals (Norton et al., 2011), and pharmacological inhibition or lesion of PPN neurons alters established addiction behavior, such as nicotine self-administration (Corrigall et al., 2002; Lanca et al., 2000). However, a causal link to a specific neuronal population in the PPN, whose modulation can affect reward behavior, has been lacking. Our results illustrate that optogenetic activation of PPN ChAT neurons lends positive emotional valence to previously aversive places (Fig. 4F–G). Conversely, inhibition of PPN ChAT neurons produces place aversion (Fig. 4H, I). Thus, PPN ChAT signaling can bidirectionally influence reinforcement learning.

A number of elegant studies have revealed complex roles for SNc and VTA neurons in exploratory activity, habituation, reinforcement, aversion, etc (Bromberg-Martin et al., 2010; Friedman et al., 2014; Lerner et al., 2015; Roeper, 2013; Walsh et al., 2014). We observed that stimulating ChAT terminals in the vSNc and VTA respectively modulate locomotion and reward (Fig. 5), suggesting that vSNc and VTA neurons receiving PPN ChAT innervation discriminately modulate locomotion and reward. Compared with the locomotor and reward phenotypes during modulation of PPN ChAT-neuron somata, terminal stimulation/inhibition tended to bring about smaller effects (Fig. 4B, C, G; Fig. 5C–F; Fig. 6F), suggesting that ChAT connections to the vSNc and VTA may only partially mediate the roles of PPN ChAT neurons in motor control and reward processing.

Similar to the PPN ChAT neurons (Fig. 1H, K, Fig. S1), LDT ChAT neurons also innervate midbrain neurons (Fig. 7D–F) through activating nAChRs on both midbrain neurons and glutamatergic terminals (Fig. 7G; Fig. S8C–D). Optogenetic stimulation of VTA projecting

LDT glutamatergic neurons has previously been found to produce place preference (Lammel et al., 2012). Here, we observed that photoexcitation of LDT-to-VTA ChAT projections produced similar effects. These dual contributions of glutamatergic and ChAT neurons to conditioned reinforcement, as well as their physiological role in generating and maintaining burst firing in VTA neurons (Chen and Lodge, 2013; Lodge and Grace, 2006), bolster the role of the LDT in reward processing. By contrast, comparatively little is known about the LDT's contribution to locomotion. Our anatomical data showed that LDT ChAT neurons also projected to the vSNc (Fig. 8C, D; Fig. S8G). However, the stimulation of these projections *in vivo* did not affect locomotion and reward processing (Fig. 7M–O). Thus, although the PPN and LDT are similar in neuronal composition, projection pathway, and their contributions to reward processing, they differ in their modulation of locomotion (Fig. 8E). These differences and similarities align with their unique anatomical features. While the percentages of VTA-projecting ChAT neurons are comparable between the PPN and the LDT, noticeably more vSNc-projecting ChAT neurons reside in the PPN (Fig. 8D, E).

Brain-wide persistent augmentation of ChAT tone by genetically enhancing the sensitivity of nicotinic acetylcholine receptors (nAChRs), the actuators of ChAT transmission, produces a hyperactivity phenotype (Drenan et al., 2008) and facilitates nicotine reward-related behaviors (Tapper et al., 2004). In contrast, the knock-out of major subtype of nAChRs eliminates nicotine self-administration (Picciotto et al., 1998). These mouse genetic studies suggest that ChAT tone plays critical roles in both locomotion and reward reinforcement. Our results extend these studies by showing that temporally precise modulation of distinct ChAT pathways, originating in the mesopontine tegmentum, can exert contrasting actions on locomotion and reward (Fig. 8E). PPN ChAT neurons regulate locomotion and reward through divergent pathways connecting to the vSNc and VTA, respectively. A parallel LDT ChAT projection pathway modulates reward alone. Therefore, to refine the therapeutic treatment of movement disorders or drug addiction, it may be advantageous to specifically target discrete mesopontine cholinergic pathways (PPN-to-vSNc for enhancing motor function, and PPN/LDT-to-VTA for curbing addiction).

Experimental procedures

We used Long Evans wild type and Choline acetyl-transferase (ChAT)-Cre rats with Long Evans background (Witten et al., 2011). Animal husbandry and all experimental procedures involving rats were approved by the Institutional Animal Care and Use Committee (IACUC) and by the Office of Laboratory Animal Resources at the California Institute of Technology.

Surgeries for viral delivery, optical fiber implantation, and retrograde tracing

The rats were anesthetized with 2% isofluorane gas/carbogen mixture and stabilized on a stereotaxic frame (Kopf Instruments). AAV5-Ef1α-DIO-ChR2-eYFP, AAV5-Ef1α-DIO-Arch3.0-eYFP, AAV5-Ef1α-DIO-eNpHR3.0-eYFP, AAV5-Ef1α-DIO-mCherry, or AAV5-Ef1α-DIO-eYFP (0.8 μL, viral concentration is $4X10^{12}$ genome copies, UNC Vector Core) was injected in the PPN or LDT of ChAT-Cre rats (3 months old), and custom-made optical fiber guides (300 μm in diameter) were implanted above virus injection sites in the PPN, or above their projection nuclei (i.e. the vSNc and the VTA). Following surgery, rats were

single-housed on a 12 hrs light/dark cycle until behavioral testing (4–6 months old) or until electrophysiological recordings (4–7 months old).

For retrograde tracing, we injected herpes simplex virus carrying eYFP- and mCherry-Cre (MIT Viral Gene Transfer Core) in the VTA and the vSNc, respectively, and allowed the rats to recover for 3 weeks before imaging eYFP and mCherry in PPN ChAT and non-ChAT neurons.

Brain slice patch-clamp recordings

Electrophysiological recordings were performed on parasagittal brain slices, using the protocol described with some modifications (Xiao et al., 2015; Ye et al., 2006) (see supplementary materials).

In vivo single-unit recordings with optrodes

ChAT-Cre rats injected with AAV5-DIO-ChR2-eYFP into the PPN were anesthetized and optrodes, made as previously described (Gradinaru et al., 2007), were inserted into the VTA to track single-unit activity of VTA neurons before, during and after photoexcitation of ChR2-expressing PPN ChAT terminals in VTA.

Immunohistochemistry

We performed immunohistochemistry with conventional histology to identify ChR2-eYFP-/Arch3.0-eYFP-positive neurons and processes, ChAT neurons, and DA neurons. To visualize optogenetically traced projections from PPN ChAT neurons to midbrain, we cleared 1–2 mm brain sections from ChR2-injected rats with PACT (Yang et al., 2014), performed immunohistochemistry to label ChR2-eYFP fibers and midbrain DA neurons (Fig. 1B, 5B), immersed the brain sections in refractive index matching solution (RIMS) in 1–2 mm deep square frames (iSpacer), and imaged the samples with a Zeiss LSM 780 confocal microscope.

Behavioral Assays

The rats with optical fiber implants were subject to open field and conditioned place preference (CPP) assays and their behaviors were acquired with a video camera controlled by Ethovision XT 9 software (Noldus et al., 2001).

Data analysis

Statistical analysis was performed by SigmaPlot 11.0 (SPSS Inc.) and OpenEpi (Dean et al., 2010). Values of $p < 0.05$ were considered significant.

Supplementary Material

Refer to Web version on PubMed Central for supplementary material.

Acknowledgments

We thank the entire Gradinaru lab for helpful discussions and Drs. David J. Anderson and Henry A. Lester for helpful comments on the manuscript. This work was supported by grants to VG: NIH Director's New Innovator

IDP20D017782-01; NIH/NIA 1R01AG047664-01 (CX is a co-investigator); NIH BRAIN 1U01NS090577; Heritage Medical Research Institute; Beckman Institute for Optogenetics and CLARITY; Pew Charitable Trust; Michael J. Fox Foundation; Sloan Foundation. Work in the Gradinaru Laboratory at Caltech is also funded by the following awards (to VG): NIH/NIMH 1R21MH103824-01; Kimmel Foundation; Human Frontiers in Science Program; Mallinckrodt Foundation; Gordon and Betty Moore Foundation through Grant GBMF2809 to the Caltech Programmable Molecular Technology Initiative; GSK Bioelectronics Research Grants; Hereditary Disease Foundation; Caltech-GIST; Caltech-Amgen; Caltech-CEMI; Caltech-City of Hope Biomedical Initiative. C.X. is partly supported by Michael J. Fox Foundation. J.B.T. acknowledges the Colvin Postdoctoral Fellowship. K.C. is supported by the NIH Predoctoral Training in Biology and Chemistry (2T32GM007616-36).

References

Antinone SE, Smith GA. Retrograde axon transport of herpes simplex virus and pseudorabies virus: a live-cell comparative analysis. Journal of virology. 2010; 84:1504–1512. [PubMed: 19923187]

Arnulf I, Ferraye M, Fraix V, Benabid AL, Chabardes S, Goetz L, Pollak P, Debu B. Sleep induced by stimulation in the human pedunculopontine nucleus area. Annals of neurology. 2010; 67:546–549. [PubMed: 20437591]

Ballanger B, Lozano AM, Moro E, van Eimeren T, Hamani C, Chen R, Cilia R, Houle S, Poon YY, Lang AE, Strafella AP. Cerebral blood flow changes induced by pedunculopontine nucleus stimulation in patients with advanced Parkinson's disease: a [(15)O] H2O PET study. Human brain mapping. 2009; 30:3901–3909. [PubMed: 19479730]

Benarroch EE. Pedunculopontine nucleus: functional organization and clinical implications. Neurology. 2013; 80:1148–1155. [PubMed: 23509047]

Bermudez MA, Schultz W. Timing in reward and decision processes. Philosophical transactions of the Royal Society of London Series B, Biological sciences. 2014; 369:20120468. [PubMed: 24446502]

Blaha CD, Allen LF, Das S, Inglis WL, Latimer MP, Vincent SR, Winn P. Modulation of dopamine efflux in the nucleus accumbens after cholinergic stimulation of the ventral tegmental area in intact, pedunculopontine tegmental nucleus-lesioned, and laterodorsal tegmental nucleus-lesioned rats. The Journal of neuroscience : the official journal of the Society for Neuroscience. 1996; 16:714–722. [PubMed: 8551354]

Bohnen NI, Frey KA, Studenski S, Kotagal V, Koeppe RA, Scott PJ, Albin RL, Muller ML. Gait speed in Parkinson disease correlates with cholinergic degeneration. Neurology. 2013; 81:1611–1616. [PubMed: 24078735]

Bohnen NI, Muller ML, Koeppe RA, Studenski SA, Kilbourn MA, Frey KA, Albin RL. History of falls in Parkinson disease is associated with reduced cholinergic activity. Neurology. 2009; 73:1670–1676. [PubMed: 19917989]

Bromberg-Martin ES, Matsumoto M, Hikosaka O. Dopamine in motivational control: rewarding, aversive, and alerting. Neuron. 2010; 68:815–834. [PubMed: 21144997]

Chen L, Lodge DJ. The lateral mesopontine tegmentum regulates both tonic and phasic activity of VTA dopamine neurons. Journal of neurophysiology. 2013; 110:2287–2294. [PubMed: 24004527]

Chow BY, Han X, Dobry AS, Qian X, Chuong AS, Li M, Henninger MA, Belfort GM, Lin Y, Monahan PE, Boyden ES. High-performance genetically targetable optical neural silencing by light-driven proton pumps. Nature. 2010; 463:98–102. [PubMed: 20054397]

Corrigall WA, Coen KM, Zhang J, Adamson L. Pharmacological manipulations of the pedunculopontine tegmental nucleus in the rat reduce self-administration of both nicotine and cocaine. Psychopharmacology (Berl). 2002; 160:198–205. [PubMed: 11875638]

Dani JA, Bertrand D. Nicotinic acetylcholine receptors and nicotinic cholinergic mechanisms of the central nervous system. Annual review of pharmacology and toxicology. 2007; 47:699–729.

Dautan D, Huerta-Ocampo I, Witten IB, Deisseroth K, Bolam JP, Gerdjikov T, Mena-Segovia J. A major external source of cholinergic innervation of the striatum and nucleus accumbens originates in the brainstem. The Journal of neuroscience : the official journal of the Society for Neuroscience. 2014; 34:4509–4518. [PubMed: 24671996]

Dean, AG.; Sullivan, KM.; Soe, MM. OpenEpi: Open Source Epidemiologic Statistics for Public Health. 2010. Version 2.3.1www.OpenEpi.com

Drenan RM, Grady SR, Whiteaker P, McClure-Begley T, McKinney S, Miwa JM, Bupp S, Heintz N, McIntosh JM, Bencherif M, et al. In vivo activation of midbrain dopamine neurons via sensitized,

high-affinity alpha 6 nicotinic acetylcholine receptors. Neuron. 2008; 60:123–136. [PubMed: 18940593]

Drenan RM, Lester HA. Insights into the neurobiology of the nicotinic cholinergic system and nicotine addiction from mice expressing nicotinic receptors harboring gain-of-function mutations. Pharmacol Rev. 2012; 64:869–879. [PubMed: 22885704]

Friedman AK, Walsh JJ, Juarez B, Ku SM, Chaudhury D, Wang J, Li X, Dietz DM, Pan N, Vialou VF, et al. Enhancing depression mechanisms in midbrain dopamine neurons achieves homeostatic resilience. Science. 2014; 344:313–319. [PubMed: 24744379]

Futami T, Takakusaki K, Kitai ST. Glutamatergic and cholinergic inputs from the pedunculopontine tegmental nucleus to dopamine neurons in the substantia nigra pars compacta. Neuroscience research. 1995; 21:331–342. [PubMed: 7777224]

Good CH, Lupica CR. Properties of distinct ventral tegmental area synapses activated via pedunculopontine or ventral tegmental area stimulation in vitro. The Journal of physiology. 2009; 587:1233–1247. [PubMed: 19188251]

Gradinaru V, Mogri M, Thompson KR, Henderson JM, Deisseroth K. Optical deconstruction of parkinsonian neural circuitry. Science. 2009; 324:354–359. [PubMed: 19299587]

Gradinaru V, Thompson KR, Zhang F, Mogri M, Kay K, Schneider MB, Deisseroth K. Targeting and readout strategies for fast optical neural control in vitro and in vivo. The Journal of neuroscience : the official journal of the Society for Neuroscience. 2007; 27:14231–14238. [PubMed: 18160630]

Gradinaru V, Zhang F, Ramakrishnan C, Mattis J, Prakash R, Diester I, Goshen I, Thompson KR, Deisseroth K. Molecular and cellular approaches for diversifying and extending optogenetics. Cell. 2010; 141:154–165. [PubMed: 20303157]

Hassan A, Benarroch EE. Heterogeneity of the midbrain dopamine system: Implications for Parkinson disease. Neurology. 2015; 85:1795–1805. [PubMed: 26475693]

Hausser M. Optogenetics: the age of light. Nature methods. 2014; 11:1012–1014. [PubMed: 25264778]

Ikemoto S. Dopamine reward circuitry: two projection systems from the ventral midbrain to the nucleus accumbens-olfactory tubercle complex. Brain Res Rev. 2007; 56:27–78. [PubMed: 17574681]

Jenkinson N, Nandi D, Miall RC, Stein JF, Aziz TZ. Pedunculopontine nucleus stimulation improves akinesia in a Parkinsonian monkey. Neuroreport. 2004; 15:2621–2624. [PubMed: 15570164]

Jenkinson N, Nandi D, Muthusamy K, Ray NJ, Gregory R, Stein JF, Aziz TZ. Anatomy, physiology, and pathophysiology of the pedunculopontine nucleus. Movement disorders : official journal of the Movement Disorder Society. 2009; 24:319–328. [PubMed: 19097193]

Jennings JH, Sparta DR, Stamatakis AM, Ung RL, Pleil KE, Kash TL, Stuber GD. Distinct extended amygdala circuits for divergent motivational states. Nature. 2013; 496:224–228. [PubMed: 23515155]

Karachi C, Grabli D, Bernard FA, Tande D, Wattiez N, Belaid H, Bardinet E, Prigent A, Nothacker HP, Hunot S, et al. Cholinergic mesencephalic neurons are involved in gait and postural disorders in Parkinson disease. The Journal of clinical investigation. 2010; 120:2745–2754. [PubMed: 20628197]

Kojima J, Yamaji Y, Matsumura M, Nambu A, Inase M, Tokuno H, Takada M, Imai H. Excitotoxic lesions of the pedunculopontine tegmental nucleus produce contralateral hemiparkinsonism in the monkey. Neuroscience letters. 1997; 226:111–114. [PubMed: 9159502]

Kravitz AV, Kreitzer AC. Striatal mechanisms underlying movement, reinforcement, and punishment. Physiology. 2012; 27:167–177. [PubMed: 22689792]

Lammel S, Lim BK, Ran C, Huang KW, Betley MJ, Tye KM, Deisseroth K, Malenka RC. Input-specific control of reward and aversion in the ventral tegmental area. Nature. 2012; 491:212–217. [PubMed: 23064228]

Lanca AJ, Adamson KL, Coen KM, Chow BL, Corrigall WA. The pedunculopontine tegmental nucleus and the role of cholinergic neurons in nicotine self-administration in the rat: a correlative neuroanatomical and behavioral study. Neuroscience. 2000; 96:735–742. [PubMed: 10727791]

Lau B, Welter ML, Belaid H, Fernandez Vidal S, Bardinet E, Grabli D, Karachi C. The integrative role of the pedunculopontine nucleus in human gait. Brain. 2015; 138:1284–1296. [PubMed: 25765327]

Lerner TN, Shilyansky C, Davidson TJ, Evans KE, Beier KT, Zalocusky KA, Crow AK, Malenka RC, Luo L, Tomer R, Deisseroth K. Intact-Brain Analyses Reveal Distinct Information Carried by SNc Dopamine Subcircuits. Cell. 2015; 162:635–647. [PubMed: 26232229]

Lodge DJ, Grace AA. The laterodorsal tegmentum is essential for burst firing of ventral tegmental area dopamine neurons. Proceedings of the National Academy of Sciences of the United States of America. 2006; 103:5167–5172. [PubMed: 16549786]

Mahn M, Prigge M, Ron S, Levy R, Yizhar O. Biophysical constraints of optogenetic inhibition at presynaptic terminals. Nature neuroscience. 2016

Marani E, Heida T, Lakke EA, Usunoff KG. The subthalamic nucleus. Part I: development, cytology, topography and connections. Adv Anat Embryol Cell Biol. 2008; 198:1–113. vii. [PubMed: 18727483]

Masdeu JC, Alampur U, Cavaliere R, Tavoulareas G. Astasia and gait failure with damage of the pontomesencephalic locomotor region. Annals of neurology. 1994; 35:619–621. [PubMed: 8179307]

Maskos U. The cholinergic mesopontine tegmentum is a relatively neglected nicotinic master modulator of the dopaminergic system: relevance to drugs of abuse and pathology. Br J Pharmacol 153 Suppl. 2008; 1:S438–445.

Mattis J, Tye KM, Ferenczi EA, Ramakrishnan C, O'Shea DJ, Prakash R, Gunaydin LA, Hyun M, Fenno LE, Gradinaru V, et al. Principles for applying optogenetic tools derived from direct comparative analysis of microbial opsins. Nature methods. 2012; 9:159–172. [PubMed: 22179551]

Mena-Segovia J, Winn P, Bolam JP. Cholinergic modulation of midbrain dopaminergic systems. Brain Res Rev. 2008; 58:265–271. [PubMed: 18343506]

Miwa JM, Freedman R, Lester HA. Neural systems governed by nicotinic acetylcholine receptors: emerging hypotheses. Neuron. 2011; 70:20–33. [PubMed: 21482353]

Morita H, Hass CJ, Moro E, Sudhyadhom A, Kumar R, Okun MS. Pedunculopontine Nucleus Stimulation: Where are We Now and What Needs to be Done to Move the Field Forward? Frontiers in neurology. 2014; 5:243. [PubMed: 25538673]

Nieh EH, Matthews GA, Allsop SA, Presbrey KN, Leppla CA, Wichmann R, Neve R, Wildes CP, Tye KM. Decoding neural circuits that control compulsive sucrose seeking. Cell. 2015; 160:528–541. [PubMed: 25635460]

Noldus LP, Spink AJ, Tegelenbosch RA. EthoVision: a versatile video tracking system for automation of behavioral experiments. Behavior research methods, instruments, & computers : a journal of the Psychonomic Society, Inc. 2001; 33:398–414.

Norton AB, Jo YS, Clark EW, Taylor CA, Mizumori SJ. Independent neural coding of reward and movement by pedunculopontine tegmental nucleus neurons in freely navigating rats. The European journal of neuroscience. 2011; 33:1885–1896. [PubMed: 21395868]

Oakman SA, Faris PL, Kerr PE, Cozzari C, Hartman BK. Distribution of pontomesencephalic cholinergic neurons projecting to substantia nigra differs significantly from those projecting to ventral tegmental area. The Journal of neuroscience : the official journal of the Society for Neuroscience. 1995; 15:5859–5869. [PubMed: 7666171]

Okada K, Kobayashi Y. Reward prediction-related increases and decreases in tonic neuronal activity of the pedunculopontine tegmental nucleus. Frontiers in integrative neuroscience. 2013; 7:36. [PubMed: 23717270]

Patterson CM, Wong JM, Leinninger GM, Allison MB, Mabrouk OS, Kasper CL, Gonzalez IE, Mackenzie A, Jones JC, Kennedy RT, Myers MG Jr. Ventral tegmental area neurotensin signaling links the lateral hypothalamus to locomotor activity and striatal dopamine efflux in male mice. Endocrinology. 2015; 156:1692–1700. [PubMed: 25734363]

Picciotto MR, Zoli M, Rimondini R, Lena C, Marubio LM, Pich EM, Fuxe K, Changeux JP. Acetylcholine receptors containing the β2 subunit are involved in the reinforcing properties of nicotine. Nature. 1998; 391:173–177. [PubMed: 9428762]

Pienaar IS, Gartside SE, Sharma P, De Paola V, Gretenkord S, Withers D, Elson JL, Dexter DT. Pharmacogenetic stimulation of cholinergic pedunculopontine neurons reverses motor deficits in a rat model of Parkinson's disease. Molecular neurodegeneration. 2015; 10:47. [PubMed: 26394842]

Plaha P, Gill SS. Bilateral deep brain stimulation of the pedunculopontine nucleus for Parkinson's disease. Neuroreport. 2005; 16:1883–1887. [PubMed: 16272872]

Roeper J. Dissecting the diversity of midbrain dopamine neurons. Trends in neurosciences. 2013; 36:336–342. [PubMed: 23582338]

Roseberry TK, Lee AM, Lalive AL, Wilbrecht L, Bonci A, Kreitzer AC. Cell-Type- Specific Control of Brainstem Locomotor Circuits by Basal Ganglia. Cell. 2016; 164:526–537. [PubMed: 26824660]

Scarnati E, Proia A, Campana E, Pacitti C. A microiontophoretic study on the nature of the putative synaptic neurotransmitter involved in the pedunculopontine-substantia nigra pars compacta excitatory pathway of the rat. Experimental brain research. Experimentelle Hirnforschung Experimentation cerebrale. 1986; 62:470–478. [PubMed: 2873047]

Stefani A, Lozano AM, Peppe A, Stanzione P, Galati S, Tropepi D, Pierantozzi M, Brusa L, Scarnati E, Mazzone P. Bilateral deep brain stimulation of the pedunculopontine and subthalamic nuclei in severe Parkinson's disease. Brain. 2007; 130:1596–1607. [PubMed: 17251240]

Sternson SM, Roth BL. Chemogenetic tools to interrogate brain functions. Annual review of neuroscience. 2014; 37:387–407.

Tapper AR, McKinney SL, Nashmi R, Schwarz J, Deshpande P, Labarca C, Whiteaker P, Marks MJ, Collins AC, Lester HA. Nicotine activation of α4* receptors: sufficient for reward, tolerance, and sensitization. Science. 2004; 306:1029–1032. [PubMed: 15528443]

Tattersall TL, Stratton PG, Coyne TJ, Cook R, Silberstein P, Silburn PA, Windels F, Sah P. Imagined gait modulates neuronal network dynamics in the human pedunculopontine nucleus. Nature neuroscience. 2014; 17:449–454. [PubMed: 24487235]

Treweek JB, Chan KY, Flytzanis NC, Yang B, Deverman BE, Greenbaum A, Lignell A, Xiao C, Cai L, Ladinsky MS, et al. Whole-body tissue stabilization and selective extractions via tissuehydrogel hybrids for high-resolution intact circuit mapping and phenotyping. Nature protocols. 2015; 10:1860–1896. [PubMed: 26492141]

Tsai HC, Zhang F, Adamantidis A, Stuber GD, Bonci A, de Lecea L, Deisseroth K. Phasic firing in dopaminergic neurons is sufficient for behavioral conditioning. Science. 2009; 324:1080–1084. [PubMed: 19389999]

Urban DJ, Roth BL. DREADDs (designer receptors exclusively activated by designer drugs): chemogenetic tools with therapeutic utility. Annual review of pharmacology and toxicology. 2015; 55:399–417.

Van Dort CJ, Zachs DP, Kenny JD, Zheng S, Goldblum RR, Gelwan NA, Ramos DM, Nolan MA, Wang K, Weng FJ, et al. Optogenetic activation of cholinergic neurons in the PPT or LDT induces REM sleep. Proceedings of the National Academy of Sciences of the United States of America. 2015; 112:584–589. [PubMed: 25548191]

Walsh JJ, Friedman AK, Sun H, Heller EA, Ku SM, Juarez B, Burnham VL, Mazei-Robison MS, Ferguson D, Golden SA, et al. Stress and CRF gate neural activation of BDNF in the mesolimbic reward pathway. Nature neuroscience. 2014; 17:27–29. [PubMed: 24270188]

Wang HL, Morales M. Pedunculopontine and laterodorsal tegmental nuclei contain distinct populations of cholinergic, glutamatergic and GABAergic neurons in the rat. The European journal of neuroscience. 2009; 29:340–358. [PubMed: 19200238]

Witten IB, Steinberg EE, Lee SY, Davidson TJ, Zalocusky KA, Brodsky M, Yizhar O, Cho SL, Gong S, Ramakrishnan C, et al. Recombinase-driver rat lines: tools, techniques, and optogenetic application to dopamine-mediated reinforcement. Neuron. 2011; 72:721–733. [PubMed: 22153370]

Xiao C, Miwa JM, Henderson BJ, Wang Y, Deshpande P, McKinney SL, Lester HA. Nicotinic receptor subtype-selective circuit patterns in the subthalamic nucleus. The Journal of neuroscience : the official journal of the Society for Neuroscience. 2015; 35:3734–3746. [PubMed: 25740504]

Yang B, Treweek JB, Kulkarni RP, Deverman BE, Chen CK, Lubeck E, Shah S, Cai L, Gradinaru V. Single-Cell Phenotyping within Transparent Intact Tissue through Whole-Body Clearing. Cell. 2014; 158:945–958. [PubMed: 25088144]

Ye JH, Zhang J, Xiao C, Kong JQ. Patch-clamp studies in the CNS illustrate a simple new method for obtaining viable neurons in rat brain slices: glycerol replacement of NaCl protects CNS neurons. J Neurosci Methods. 2006; 158:251–259. [PubMed: 16842860]

Yeomans JS. Role of tegmental cholinergic neurons in dopaminergic activation, antimuscarinic psychosis and schizophrenia. Neuropsychopharmacology. 1995; 12:3–16. [PubMed: 7766284]

Highlights

- Optogenetic characterization of mesopontine cholinergic cells inputs to midbrain
- Separable pedunculopontine cholinergic pathways govern locomotion and reward
- Laterodorsal tegmental cholinergic inputs to VTA modulates reward
- Retrograde tracing reveals mesopontine cholinergic collateralization to VTA and SNc

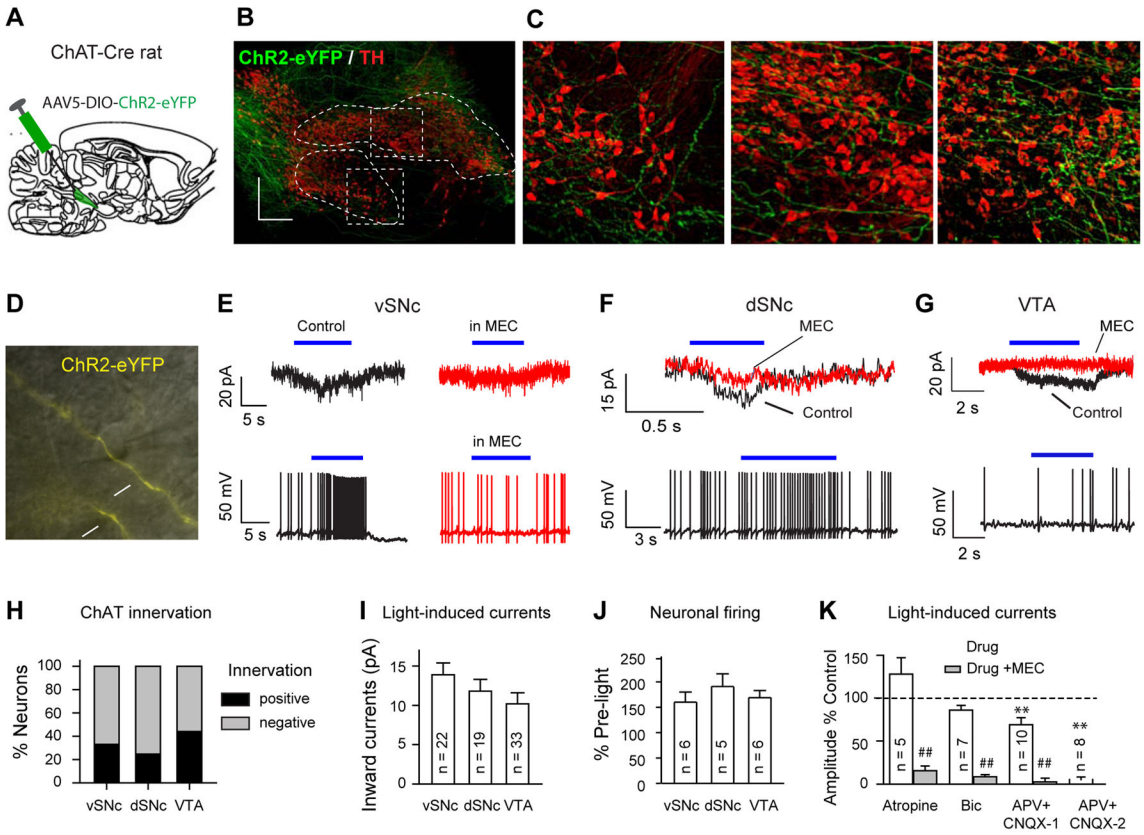

Fig. 1. PPN ChAT neurons form functional connections with distinct midbrain areas

(A) Stereotaxic microinjection of AAV5, carrying Ef1α-DIO-ChR2-eYFP, in the PPN of ChAT-Cre rats. **(B)** Representative Images from a 0.8 mm thick parasagittal midbrain section cleared with PACT and immune-stained for green fluorescent protein (ChR2-eYFP) and tyrosine hydroxylase (TH). **(C)** Expanded views of the vSNc and dSNc from **(B)**. VTA image was from a more medial section. **(D)** Brain-slice recordings were performed on midbrain neurons. The neurons were selected by their location in the vSNc, dSNc, or VTA, and their proximity to ChR2-positive fibers (arrows). **(E–G)** Blue light stimulation induced inward currents in vSNc**,** dSNc, and VTA neurons (upper traces), and consequently enhanced firing (lower traces in **E–G)**. Blue-light-evoked inward currents **(E, F)** and firing increases **(E**) were blocked by 10 μM MEC. **(H)** Percentages of neurons in the vSNc (33%, 22/66), VTA (44%, 33/76), and dSNc (24.7%, 19/58) having responses to blue light. Black and gray stacks indicate the percentages of neurons responding or not responding to light stimulation, respectively. **(I)** Summary of light-evoked inward currents in vSNc (13.9±1.5 pA), dSNc (11.8±1.5 pA), and VTA neurons (10.2±1.4 pA) (one-way ANOVA: $F_{(2)}$=1.59, p=0.22). Numbers of recorded neurons are shown in the blank bars. **(J)** Summary of light enhancement of firing rates in vSNc (160±20% of baseline), dSNc (191±25% of baseline), and VTA neurons (169±14% of baseline) (one-way ANOVA: $F_{(2)}$ = 0.58, p = 0.58). **(K)** Summary of the effects of 1 μM atropine (128±19%), 10 μM Bic (86±5.5)%, 50 μM APV and 20 μM CNQX (APV+CNQX_1, partial blocking, 69±8.2%; APV+CNQX_2, complete blocking, 5±3%) on photo-currents. Compared with control: * p<0.05; ** p<0.01; Compared with Drug only: ##: p<0.01.

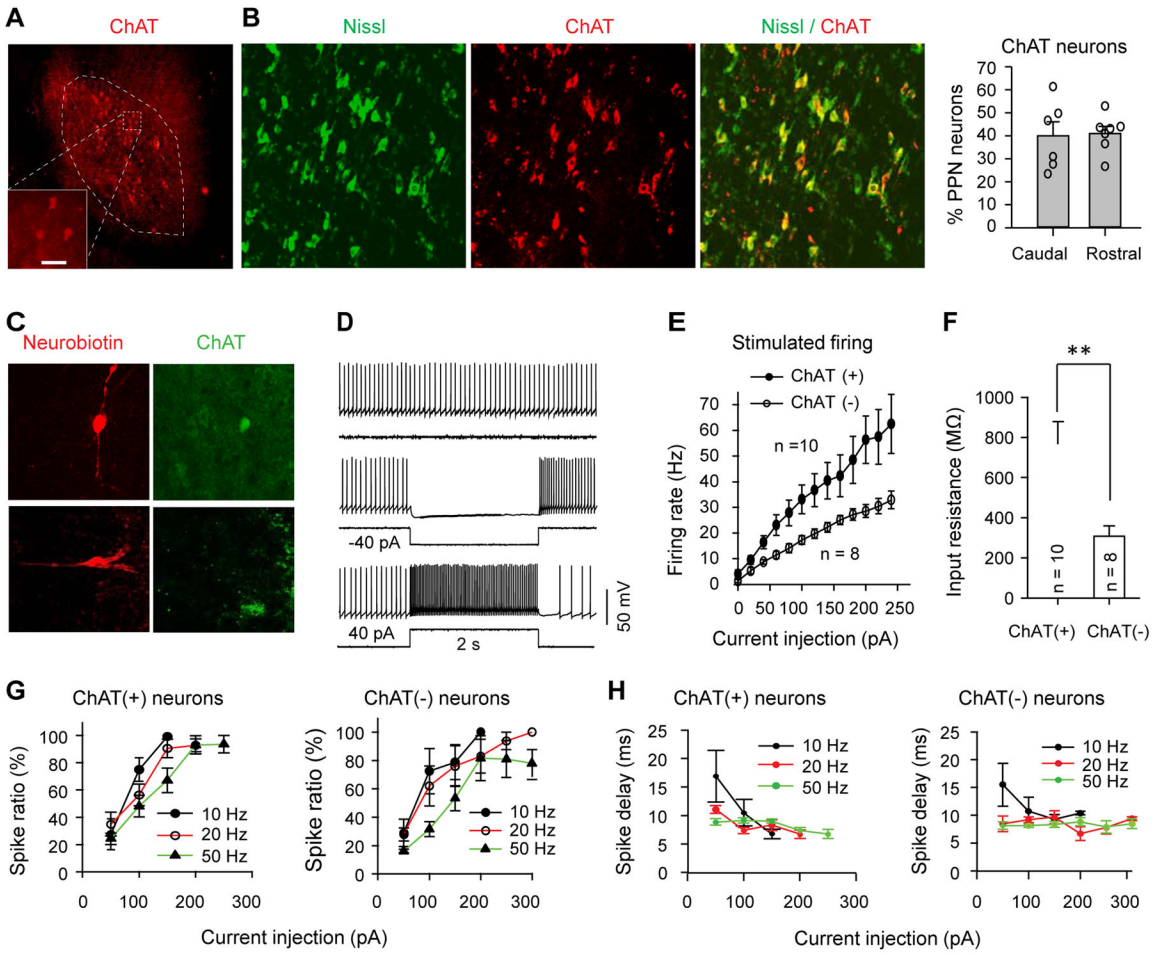

Fig. 2. Biophysical properties of PPN ChAT neurons

(A) ChAT antibody staining in the PPN. **(B)** About 40% of PPN neurons are cholinergic (representative images; summary data t-test: p=0.86). **(C)** Typical neurobiotin labeled ChAT (upper panels) and non-ChAT (lower panels) neurons. **(D)** The activity of PPN neurons was modulated by current injections. **(E)** The averaged firing rate of PPN neurons in responses to 2 s current injections. Data shown as means ± standard errors of the means. **(F)** Input resistance of PPN neurons (ChAT: 766±113 MΩ; non-ChAT: 308±52 MΩ, t-test: t=3.18, p=0.005). **(G)** The success rate of stimulus-evoked spikes (spike ratio) approached saturating levels when the injection currents were increased. **(H)** The spike delays after the initiation of current injections varied with stimulation frequency. **(G)** and **(H)** include data from 10 ChAT neurons and 8 non-ChAT neurons.

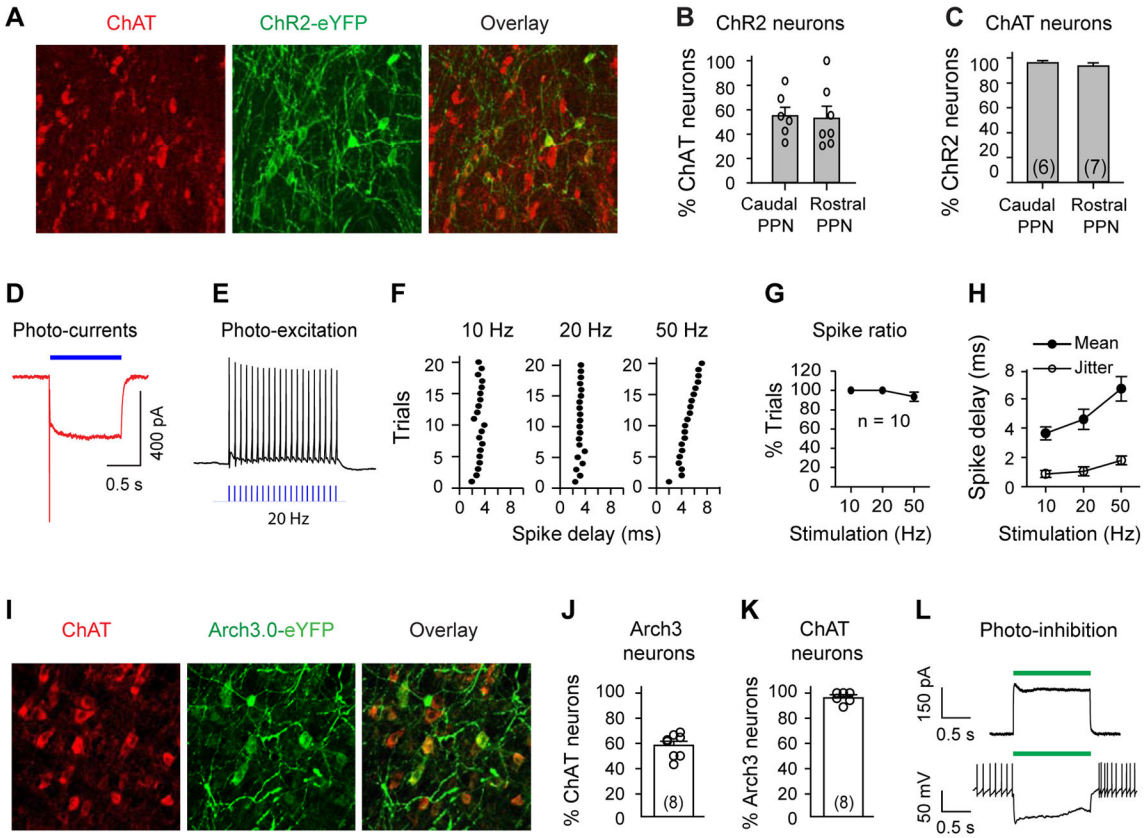

Fig. 3. Optogenetic modulation of PPN ChAT neurons

(A) ChR2-eYFP-positive neurons (green) were ChAT-positive (red). **(B)** Percentages of ChAT neurons that were transduced with ChR2-eYFP (Caudal: 55±7%; Rostral: 53±10%; *t*-test, t=0.17, p=0.87). The sections are from 3 rats (2–3 from each). **(C)** ChR2-eYFP was specifically transduced into ChAT neurons (Caudal: 96±2%; Rostral: 94±3%; t-test, t=0.93, p=0.37). **(D)** Blue light (3.1 mW/mm^2) evoked inward currents in a ChR2-positive neuron (V_H=−50 mV). **(E)** 20 Hz blue light stimuli evoked spikes in a ChR2-positive PPN neuron. **(F)** Scatter plots of spike delay for 20 trials of light-stimulation at 10, 20, and 50 Hz. **(G)** Success rate of light-evoked spikes. **(H)** Summary of the mean and variation (jitter) of spike delay. **(I)** AAV5-DIO-Arch3.0-eYFP was delivered to the PPN of ChAT-Cre rats. Arch-eYFP-positive neurons were ChAT-positive. **(J)** Arch3.0-eYFP was transduced into ~60% of ChAT neurons. **(K)** >95% of Arch3.0-eYFP-positive neurons were ChAT neurons. **(L)** Green light (9 mW/mm^2) induced an outward current (upper, V_H=−50 mV), and silenced activity (lower) in Arch3.0-containing neurons (see also Fig. S3D).

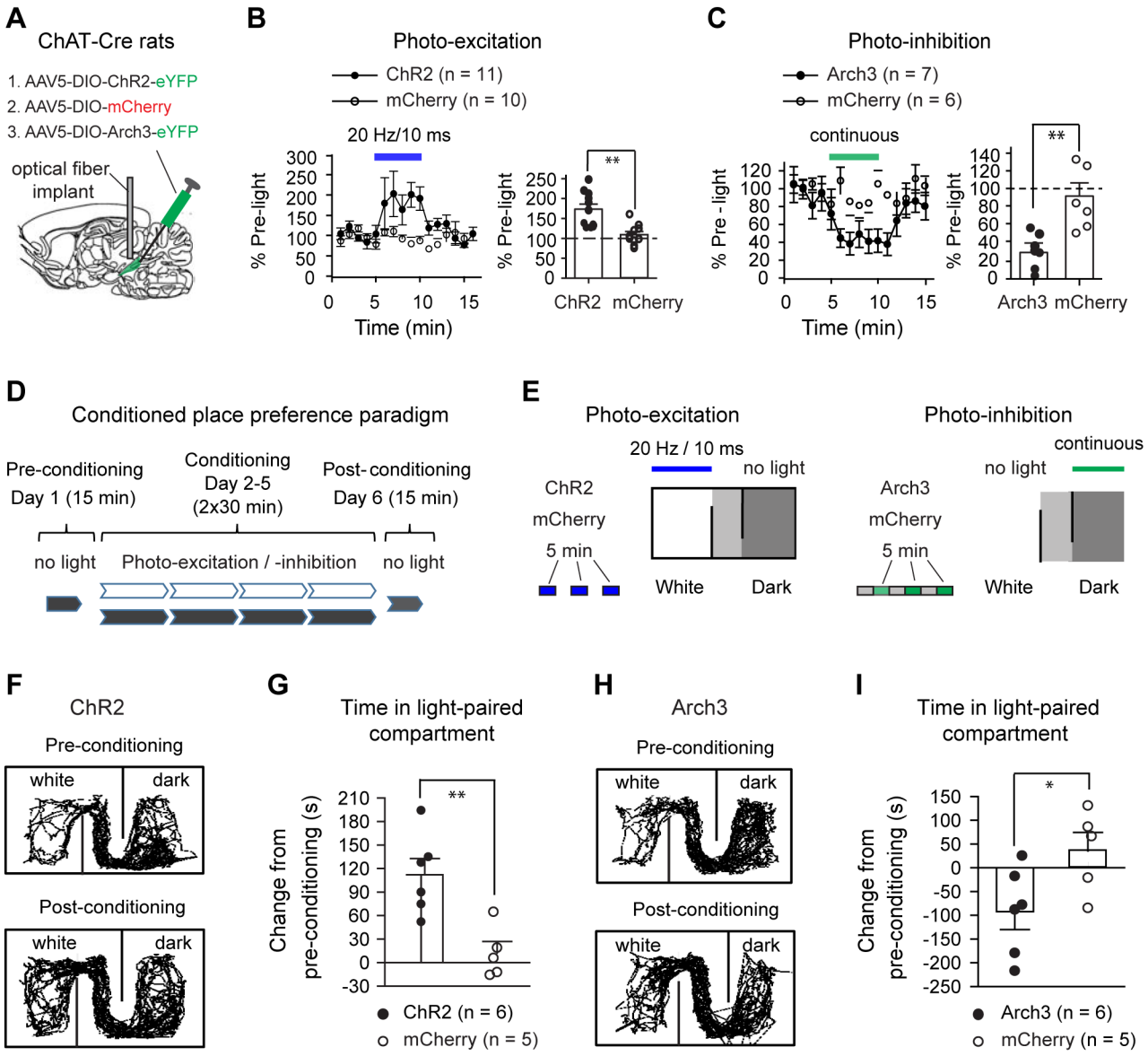

Fig. 4. PPN ChAT neurons regulate locomotion and reward

(A) AAV5 was used to transduce EF1α-DIO-ChR2-eYFP (ChR2), EF1α-DIO-Arch3.0-eYFP (Arch3), or EF1α-DIO-mCherry (mCherry) into the PPN of ChAT-Cre rats. **(B)** Blue light reversibly increased voluntary movement in ChR2 rats, but not in mCherry rats (left, time course; right, summarized effects (ChR2: 173±13%; mCherry: 109±8%; Mann-Whitney U test, p=0.001). **(C)** Green light reversibly reduced movement in Arch3 rats, but not in mCherry rats (left, time course; right, summarized effects (Arch3: 30±8%; mCherry: 94±15%, Mann-Whitney U test, p=0.001)). **(D)** The conditioned place preference paradigm included a first-day baseline preference test, two 30 min conditioning sessions (light conditioning in the morning and no-light control in the afternoon) per day for four consecutive days, and a post-conditioning preference test. **(E)** During the light-conditioning sessions, ChR2 or mCherry rats were kept in the white compartment and received 20 Hz

blue light stimuli (left); Arch3/mCherry rats were kept in the dark compartment and conditioned with continuous green light (right). Blue and green lights were applied for 5 min epoch every 10 min. **(F–G)** Blue light conditioning increased the time that ChR2 rats, but not mCherry rats, spent in the white compartment **(F**, typical movement tracks before and after conditioning; **G**, summary of time changes (ChR2: 112±21 s; mCherry: 12±15 s, *t*-test, p=0.004)**). (H–I)** Green light conditioning reduced the time that Arch3 rats spent in the dark compartment **(H**, typical movement tracks before and after conditioning; **I**, summary of time changes (Arch3: −97±35 s; mCherry: 35±34 s, *t*-test, p=0.021). * p<0.05; ** p<0.01.

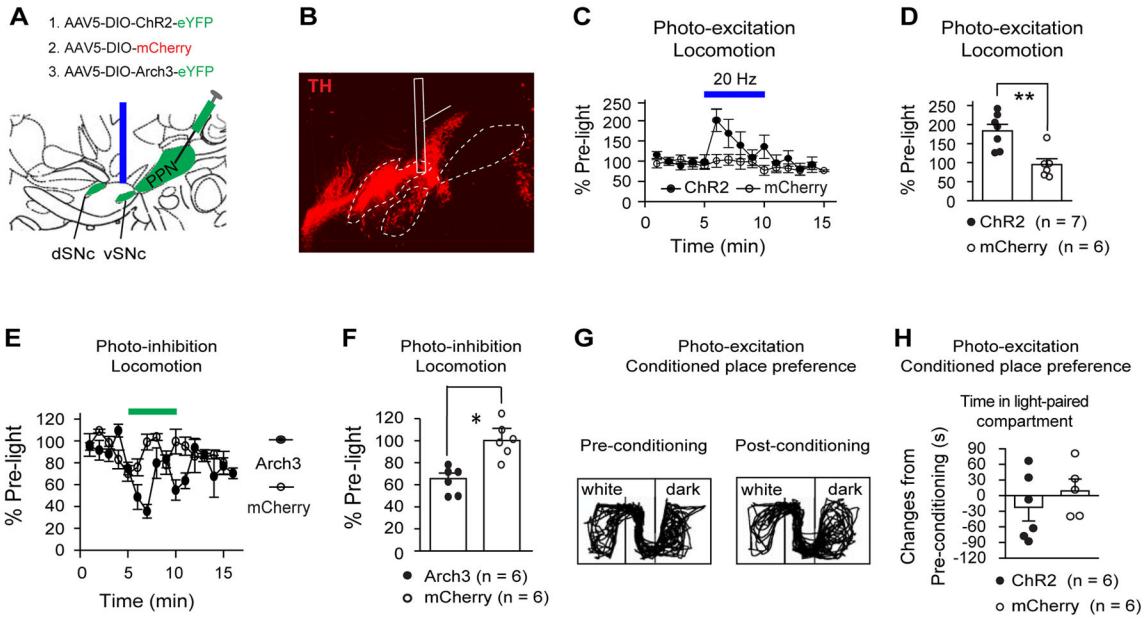

Fig. 5. Optogenetic modulation of PPN ChAT terminals in the vSNc affects locomotion

(A) Optical fibers were implanted above the vSNc to activate (AAV5-DIO-ChR2-eYFP) or inhibit (AAV5-DIO-Arch3-eYFP) PPN–vSNc ChAT projections (parasagittal plane). **(B)** A parasagittal section (1 mm) from a ChR2 rat was cleared with PACT and stained with TH antibody. **(C–D)** Photo-excitation of PPN–vSNc ChAT terminals induced locomotor enhancement **(C**, time course; **D**, summary: (ChR2: 183±17%; mCherry: 95±15%, *t*-test, p=0.003)**). (E–F)** Photo-inhibition of PPN–vSNc ChAT terminals reduced locomotion **(E**, time course; **F**, summary: Arch3: 66±5%; mCherry: 100±11%; *t*-test: t=2.66, p=0.03). **(G–H)** Photo-excitation of PPN-vSNc connections did not change CPP **(G**, typical exploration tracks in CPP chamber before and after photo-conditioning; **H**, summary of time changes in light-paired compartment (white compartment): ChR2: −22±26 s; mCherry: 9±23 s; *t*-test, p=0.40). * p<0.05; ** p<0.01.

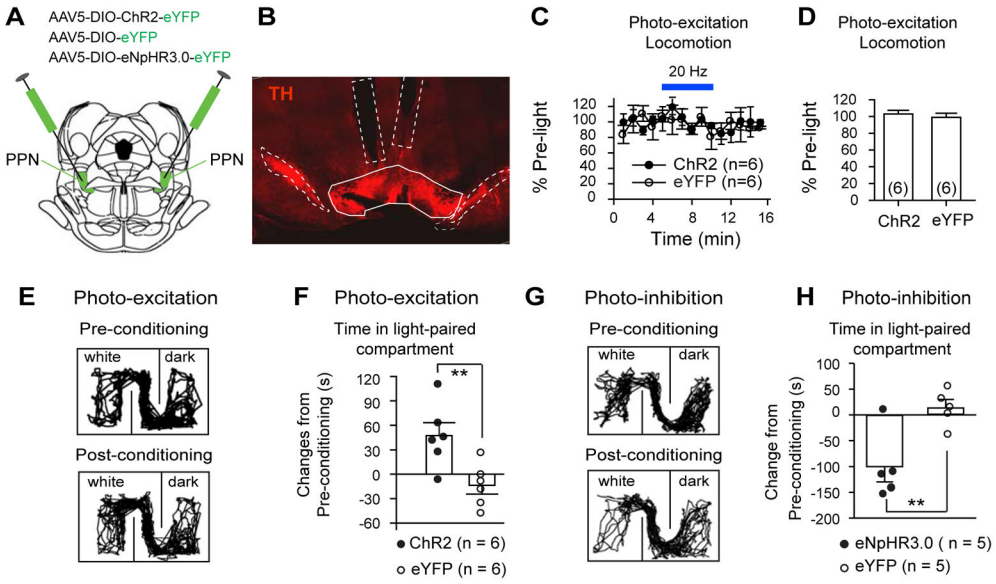

Fig. 6. Optogenetic modulation of PPN ChAT terminals in the VTA affects place preference

(A) ChR2-eYFP, eYFP, or eNpHR3.0-eYFP were virally transduced in PPN ChAT neurons of ChAT-Cre rats (coronal plane). **(B)** Optical fiber implants with a 10º angle relative to the dorsal-ventral axis were bilaterally placed above the VTA (coronal section). **(C–D**) Photo-excitation of PPN–VTA ChAT projections did not change locomotion **(C**, time course; **D**, summary: ChR2: 103±4.3%; eYFP: 99±4.9%; *t*-test, p=0.67**). (E–F)** Photo-excitation of PPN–VTA ChAT projections increased time that the rats spent in light-paired compartment **(E**, typical exploration tracks in CPP chamber before and after photo-conditioning; **F**, summary: ChR2: 47±16 s; eYFP: −14±11 s; *t*-test, p=0.01**). (G–H)** Conditioning rats with photo-inhibition of PPN-VTA ChAT projections reduced their time spent in conditioned compartment (**G**, typical exploration tracks in CPP chamber before and after photo-conditioning; **H**, summary: eNpHR3.0: −101±29 s; eYFP: 14.2±15.6 s; *t*-test, t=3.48, p=0.01). ** p<0.01.

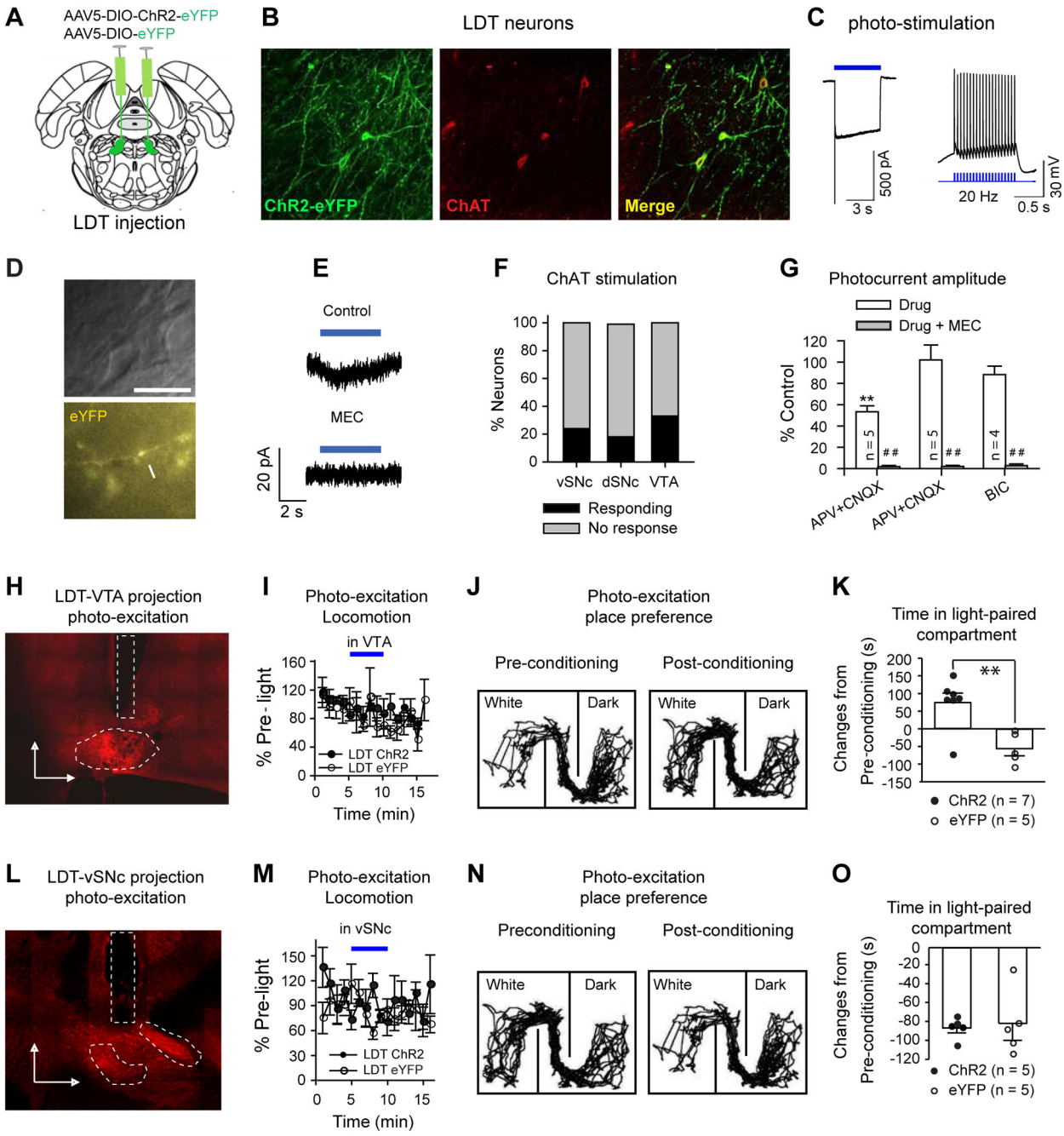

Fig. 7. Optogenetic stimulation of LDT-to-midbrain connections regulates CPP, but not locomotion

(A) AAV5-DIO-ChR2-eYFP or AAV5-DIO-eYFP was bilaterally injected in the LDT. **(B)** Typical images showing that ChR2-eYFP was selectively transduced in most LDT ChAT neurons. In 8 slices from 3 animals, 66% (368/556) of LDT ChAT neurons contained ChR2-eYFP. **(C)** Blue light (3.1 mw/mm^2) induced a robust inward current (5 s constant light) (V_H=−50 mV) and reliably evoked spikes at 20 Hz (10 ms pulses). **(D)** Typical images showing a vSNc neuron (upper panel) adjacent to a ChR2 eYFP-positive fiber (lower panel).

(E) Blue light (5 s, 3.1 mw/mm^2) evoked a MEC-sensitive inward current in a vSNc neuron (V_H=−50 mV). **(F)** Blue light respectively induced inward currents in 24% (6/25), 18% (3/17), and 33% (13/39) of neurons in the vSNc, dSNc, and VTA. Chi Square test: χ^2=1.66, p=0.44. **(G)** The photo-currents were partially blocked by APV+CNQX in some neurons, but not inhibited by either APV+CNQX or Bic in other neurons. These currents were completely abolished after addition of MEC. Drug vs. Control: ** p<0.01; Drug+MEC vs. Drug: ## p<0.01. **(H)** A typical image showing the position of implants in the VTA (in a parasagittal plane). **(I)** photo-excitation of LDT-to-VTA projections did not change locomotion. **(J–K)** Photo-excitation of LDT-to-VTA projections increased time spent in light-paired compartment (**J**, typical track tracing; **K**, summary of time changes in light-paired (white) compartment after conditioning: ChR2: 75±26 s; eYFP: −57±20 s; t-test, t=3.7, p=0.004). **(L)** A typical image showing the position of implants in the vSNc (a parasagittal plane). **(M)** Photo-excitation of LDT-to-vSNc ChAT projections did not change locomotion. **(N–O)** Conditioning rats with photo-excitation of LDT-to-vSNc projections did not change the time spent in light-paired compartment (**N**, typical track tracing; **O**, summary of time changes in light-paired compartment after conditioning (ChR2: −87±5 s; eYFP: 82±15 s; t-test, t=0.27, p=0.79).

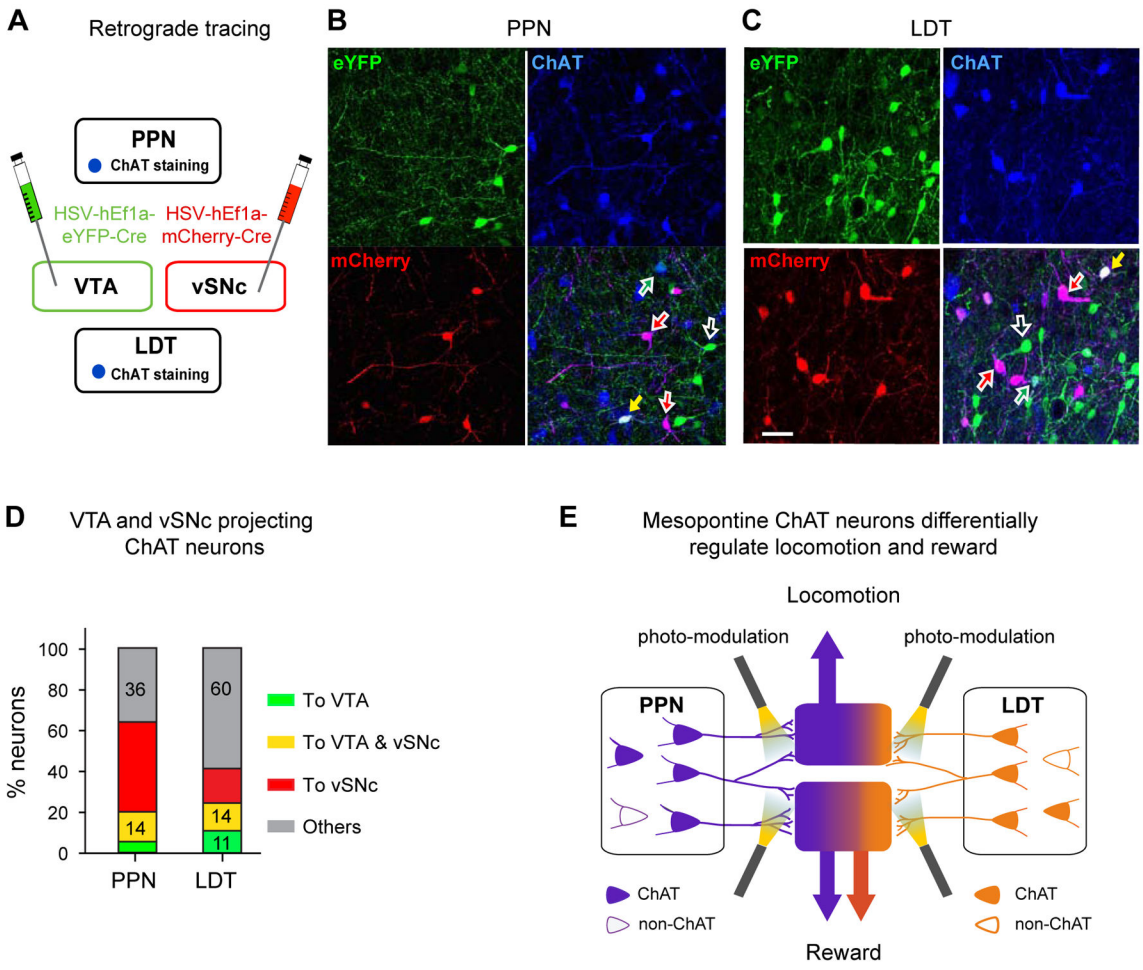

Figure 8. Retrograde tracing of PPN and LDT ChAT neurons from the VTA and vSNc

(A) The diagram shows that HSV-hEf1α-DIO-eYFP and HSV-hEf1α-DIO-mCherry are respectively injected in the VTA and vSNc. **(B, C)** Considerable proportions of ChAT and non-ChAT neurons in both the PPN **(B)** and LDT **(C)** were retrogradely labeled. Colored neurons (Green: VTA projecting neurons; Red: vSNc projecting neurons; Blue: ChAT staining); Colored arrows (green: VTA projection ChAT neuron; red: vSNc projecting ChAT neuron; yellow: ChAT neuron projecting to both the VTA and vSNc; open white arrow: non-ChAT neurons). **(D)** Percentages of PPN and LDT ChAT neurons that projected to the VTA only (green stacks), the vSNc only (red stacks), both the VTA and vSNc (yellow stacks), and neither the VTA nor the vSNc (gray stacks). A total of 484 PPN ChAT neurons and 435 LDT ChAT neurons were counted. **(E)** PPN and LDT ChAT neurons form connections with VTA neurons to a similar extent, and both modulate reward behavior; PPN ChAT neurons form stronger connections with vSNc neurons than LDT neurons do; excitation of PPN-vSNc, instead of LDT-vSNc, ChAT terminals regulates locomotion. The PPN and LDT neurons are respectively marked with green and orange (solid: ChAT; open: non-ChAT).